

Hybrid Tensor Decomposition in Neural Network Compression

Bijiao Wu^{a,*,1}, Dingheng Wang^{a,*,2}, Guangshe Zhao^{a,*,3}, Lei Deng^{b,4} and Guoqi Li^{c,*,5}

^a*School of Electronic and Information Engineering, Xi'an Jiaotong University, Xi'an 710049, China*

^b*University of California, Santa Barbara, CA93106, USA*

^c*Department of Precision Instrumentation, Center for Brain Inspired Computing Research and Beijing Innovation Center for Future Chip, Tsinghua University, Beijing 100084, China*

ARTICLE INFO

Keywords:

Neural Network Compression
Hybrid Tensor Decomposition
Hierarchical Tucker
Tensor-Train
Balanced Structure

ABSTRACT

Deep neural networks (DNNs) have enabled impressive breakthroughs in various artificial intelligence (AI) applications recently due to its capability of learning high-level features from big data. However, the current demand of DNNs for computational resources especially the storage consumption is growing due to that the increasing sizes of models are being required for more and more complicated applications. To address this problem, several tensor decomposition methods including tensor-train (TT) and tensor-ring (TR) have been applied to compress DNNs and shown considerable compression effectiveness. In this work, we introduce the hierarchical Tucker (HT), a classical but rarely-used tensor decomposition method, to investigate its capability in neural network compression. We convert the weight matrices and convolutional kernels to both HT and TT formats for comparative study, since the latter is the most widely used decomposition method and the variant of HT. We further theoretically and experimentally discover that the HT format has better performance on compressing weight matrices, while the TT format is more suited for compressing convolutional kernels. Based on this phenomenon we propose a strategy of hybrid tensor decomposition by combining TT and HT together to compress convolutional and fully connected parts separately and attain better accuracy than only using the TT or HT format on convolutional neural networks (CNNs). Our work illuminates the prospects of hybrid tensor decomposition for neural network compression.

1. Introduction

Deep neural networks (DNNs) have shown the state-of-the-art performance on many issues such as computer vision (Krizhevsky et al., 2012; He et al., 2016), natural language processing (Chen et al., 2017; Sutskever et al., 2014), reinforcement learning (Mnih et al., 2015) and many other multidisciplinary fields (Heess et al., 2015). These advanced techniques come largely from available datasets, developed algorithms and powerful CPU & GPU devices. However, as the deep learning problems become more and more complex, huge data and super large-scale DNNs become inevitable. Meanwhile, the expensive hardware cost and long processing time further complicate the deployment of DNNs on resource constrained devices.

Hence, a large number of works (Deng et al., 2020), mainly including quantization (Vanhoecke and Mao, 2011; Wu et al., 2018), pruning (Srinivas and Babu, 2015; Zhu and Gupta, 2018), knowledge distillation (Hinton et al., 2014), compact convolutional filters (Wu et al., 2017) and low-rank factorization (Novikov et al., 2015), have been investigated to reduce the hardware requirements and the running time of the deployment and application of DNNs. Among these principal approaches, low-rank factorization, which tensorizes and decomposes the weight matrices into a series of low-rank tensors with the tensor decomposition theory

originated with Hitchcock (1927), has specific advantages because of its solid mathematical theory and concise implementation. The relationship between neural networks and the tensor theory provides theoretical support for DNNs on one hand (Cohen et al., 2016), and enables the theory to be effectively applied in practical problems on the other hand (Cohen and Shashua, 2016). Consequently, several low-rank decomposition methods for compressing DNNs have attracted attention of many researchers in recent years.

As two of the most classical decomposition methods, CANDECOMP/PARAFAC (CP) (Carroll and Chang, 1970) and Tucker decomposition (Tucker, 1966) are earlier used to accelerate and compress convolutional neural networks (CNNs) (Kim et al., 2016; Lebedev et al., 2015). With the development of the tensor decomposition theory, some new methods have achieved better results in various applications. The tensor-train (TT), which is first introduced by Oseledets (2011), decomposes a high-dimensional tensor into a series of 3-dimensional tensors. Novikov et al. (2015) show that TT can reduce redundancy of DNNs by compressing the dense weight matrices in fully connected (FC) layers. Based on this, Garipov et al. (2016) extend TT to convolutional kernels to compress the whole CNNs. In recent years, researchers have attempted to improve the memory (Huang and Yu, 2018) and the energy efficiency (Deng et al., 2019) of DNNs by further boosting the application of TT decomposition. By contrast, some researchers focus on some other tensor decomposition methods for compressing DNNs with different architectures, especially recurrent neural networks (RNNs). For example, the block-term decomposition (BTD) (De Lathauwer, 2008), which decomposes a high-dimensional tensor to a sum of multiple blocks

*These authors contributed equally to this work

**Corresponding authors

¹wbj123@stu.xjtu.edu.cn

²wangdai11@stu.xjtu.edu.cn

³zhaogs@mail.xjtu.edu.cn

⁴leideng@ucsb.edu

⁵liguoqi@mail.tsinghua.edu.cn

in Tucker format, greatly reduces the parameters of RNNs and improves their training effectiveness (Ye et al., 2017). As a derived format, tensor-ring (TR) (Zhao et al., 2019) exceeds TT in performance on RNNs and achieves promising results for video classification (Pan et al., 2018). The most considerable physical significance of all of these decomposition methods mentioned above in actual is to achieve the sparse representation of the redundant weights. Naturally, the ability of each tensor decomposition method to represent high-dimensional data determines the performance of the corresponding compressed DNNs. Doubtlessly, there are obvious differences among the inner structures of different decomposition methods, which might be one of the most important reasons that affects the expressive ability of compressed DNNs, but till now is rarely discussed by previous researchers.

In this work, inspired by above studies, the flexible structure of the hierarchical Tucker (HT) decomposition method (Grasedyck and Lars, 2010), which iteratively factorizes a tensor into two subtensors by using Tucker and in actual is the source of TT, has aroused our interest. Since factorizing a tensor each time has more than one way, e.g., a tensor $\mathcal{A} \in \mathbb{R}^{n_1 \times n_2 \times n_3 \times n_4}$ whose modes could be factorized as $n_1 n_2 \times n_3 n_4$ or $n_1 \times n_2 n_3 n_4$, there are certainly multiple specific patterns for any single tensor. Therefore, the strong ability of HT to express high-dimensional data is derived from its varying structures. In general, these structures are treelike that mainly include two frequently-used patterns, namely balanced tree and degenerate tree. Moreover, researchers (Grasedyck and Hackbusch, 2011) have suggested that the balanced form of HT may require a lower rank than TT which is actually the degenerate tree form of HT. Therefore, we mainly focus on HT with balanced tree in compressing DNNs. In the rest of this paper, we only refer HT to the balanced tree unless otherwise indicated.

In our specific practices, we apply HT decomposition to compress both fully connected (FC) layers and convolutional kernels. Moreover, we compare the compressed DNNs in HT format with those in TT format under theoretical analyses and extensive experiments, and the characteristics of compression performance of these two kinds of formats are also studied. An important discovery is that the HT and TT format have respective advantages in compressing different structures of DNNs, i.e., the HT format gains better performance in compressing the weight matrices in FC layers, while the TT format is more suited for compressing convolutional kernels. We analyze and infer that the reason underlying this phenomenon is that HT prefers the tensor with balanced lengths of dimensions, while it is better for TT to compress the tensor with unbalanced dimensions. Based on this we propose a hybrid compression strategy consisting of TT-decomposed convolutional and HT-decomposed FC layers to improve the overall compression performance. The results of our experiments verify the effectiveness of the proposed method.

The main contributions of this work are summarized as follows:

- It is the first time for HT decomposition being applied to compress DNNs to the best of our knowledge, and we experimentally show that HT has comparable compression ability to TT.
- We claim that HT is more sensitive than TT to the unbalanced tensor shape during gradient descending based on the theoretical analysis of the training process.
- We propose a strategy of hybrid tensor decomposition, in which HT and TT are separately applied in FC layers and convolutional kernels, outperforming using either of HT or TT.
- Our work enlightens to select the best tensorized strategy for specific DNNs and even design new neural architectures, which makes a step forward in deploying DNNs on embedded devices.

The rest of this paper is organized as follows. In Section 2, we mainly introduce DNNs in the HT format. In Section 3, we analyze the different advantages of HT- and TT-decomposed networks and propose a strategy of hybrid tensor decomposition which is further verified by our experiments in Section 4. Section 5 discusses some complex and interesting phenomena of our experiments. Finally, we give our conclusion in Section 6.

2. DNNs in the HT Format

In this section, we give three presentations of HT decomposition, i.e., basic, normal and contracted forms, all of which can replace the original uncompressed weights and rewrite the mapping from input signals to output signals. We also introduce the relationship between HT and TT, of which the latter is derived from the former.

2.1. HT Decomposition

2.1.1. Basic Form

The hierarchical tensor format is introduced by Hackbusch and KÄijhn (2009), and on this basis Grasedyck and Lars (2010) propose the HT decomposition. For a tensor $\mathcal{A} \in \mathbb{R}^{n_1 \times n_2 \times \dots \times n_d}$, we can divide the dimensions into two sets, i.e., $t = \{t_1, t_2, \dots, t_k\}$ and $s = \{s_1, s_2, \dots, s_{d-k}\}$, to produce a matricization of \mathcal{A} like $A^{(t)} \in \mathbb{R}^{n_{t_1} n_{t_2} \dots n_{t_k} \times n_{s_1} n_{s_2} \dots n_{s_{d-k}}}$. Similarly, set t can also be grouped into t_l and t_v , to obtain other two matrices $A^{(t_l)}$ and $A^{(t_v)}$. If we define their corresponding column basis matrices as U_t, U_{t_l}, U_{t_v} , we could have (Kressner and Tobler, 2011):

$$U_t = (U_{t_l} \otimes U_{t_v}) B_t, \quad (1)$$

where $U_t \in \mathbb{R}^{n_{t_1} n_{t_2} \dots n_{t_k} \times r_t}$, $U_{t_l} \in \mathbb{R}^{n_{t_{l_1}} n_{t_{l_2}} \dots n_{t_{l_i}} \times r_{t_l}}$, $U_{t_v} \in \mathbb{R}^{n_{t_{v_1}} n_{t_{v_2}} \dots n_{t_{v_{k-i}}} \times r_{t_v}}$ are called truncated matrices, and $B_t \in \mathbb{R}^{r_{t_l} r_{t_v} \times r_t}$ is termed as transfer matrix. All the r_t, r_{t_l}, r_{t_v} are referred to as ranks. Besides, the operator \otimes represents Kronecker product.

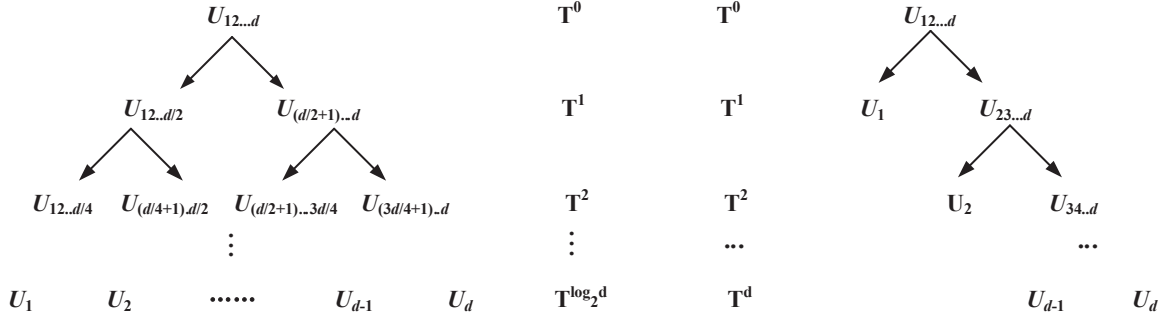


Figure 1: Dimension tree. Left: balanced tree of HT. $d = 2^k$ ($k = 1, 2, 3, \dots$). Right: degenerate tree of TT.

By iteratively using Equation (1) until all the rest truncated matrices cannot be further decomposed, the final structure of HT will come out. This process for \mathcal{A} can be generally expressed as follows:

$$\begin{aligned} \mathcal{A} \rightarrow U_{12\dots d} &= (U_{12\dots d/2} \otimes U_{(d/2+1)\dots d}) B_{12\dots d} \\ &= [(U_{12\dots d/4} \otimes U_{(d/4+1)\dots d/2}) B_{12\dots d/2}] \\ &\quad \otimes [(U_{(d/2+1)\dots 3d/4} \otimes U_{(3d/4+1)\dots d}) \\ &\quad \quad B_{(d/2+1)\dots d}] B_{12\dots d} \\ &= \dots, \end{aligned} \quad (2)$$

where $U_{12\dots d} \in \mathbb{R}^{n_1 n_2 \dots n_d \times 1}$ is reshaped from the tensor \mathcal{A} and the last ellipsis represents the subsequent decomposition of the tensor. Such presentation is called the *basic form* of the HT format, which can be drawn as a dimension tree made up of d truncated matrices and $d - 1$ transfer matrices illustrated in Figure 1.

2.1.2. Normal Form

It is obvious that Equation (2) is not very regular and simple to apply. In fact, it is easily observed that when the HT process is finished, d truncated matrices will have only one corner mark, i.e., U_1, U_2, \dots, U_d . By using a common law “ $AB \otimes CD = (A \otimes C)(B \otimes D)$ ”, one can obtain a more concise HT format from Equation (2) like (Kressner and Tobler, 2011):

$$U_{12\dots d} = (U_1 \otimes U_2 \otimes \dots \otimes U_d) (B_{12} \otimes B_{34} \otimes \dots \otimes B_{(d-1)d}) \dots B_{12\dots d}, \quad (3)$$

which is called the *normal form* of HT since it is used more widely in tradition (Hou and Chaib-draa, 2015; Kressner and Tobler, 2011, 2014). The most remarkable characteristic of this form is that the calculation is arranged as level-to-level in the perspective of the dimension tree. Thus one can directly design HT in the normal form for a tensor without iteratively calling Equation (1).

2.1.3. Contracted Form

On the other hand, the so called dimension tree in Figure 1 is actually a kind of tensor network graph (Espig et al.,

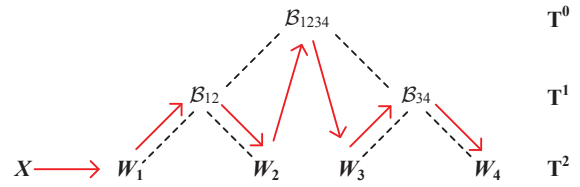


Figure 2: The order of chain computation in a case of 4-dimensional tensor. The arrows represent the order of computation. X represents the input data, B_i is the tensorized transfer matrix produced by each decomposition, and W_i is the truncated matrix.

2011), since any two matrices in the dimension tree can be merged as one by using a contraction operator. In detail, if we reshape $B_i \in \mathbb{R}^{r_{i1} r_{i2} \dots r_{id} \times r_i}$ in Equation (1) as a 3-dimensional tensor $B_i \in \mathbb{R}^{r_{i1} \times r_{i2} \times r_i}$, we can have:

$$U_i = U_{t_i} \times^1 B_i \times^1 U_{t_v}, \quad (4)$$

where \times^1 is called mode-1 contracted product (Lee and Cichocki, 2016). Then iteratively using this formulation, a new form to rewrite Equation (2) or (3) should be:

$$\begin{aligned} U_{12\dots d} &= (\dots ((U_1 \times^1 B_{12} \times^1 U_2) \times^1 B_{1234} \times^1 \\ &\quad (U_3 \times^1 B_{34} \times^1 U_4)) \times^1 \dots \times^1 \\ &\quad (U_{(d-1)} \times^1 B_{(d-1)d} \times^1 U_d) \dots), \end{aligned} \quad (5)$$

which is termed as the *contracted form* of HT.

In this way, the expensive Kronecker product is avoided, thus the corresponding calculation process and probable middle results may not consume very high computation and storage costs. For example, the contracted form of HT can allow an external input tensor to calculate with its truncated and transfer matrices one by one as shown in Figure 2, which appears to be the most efficient way that Equation (2) and (3) cannot match.

2.2. HT-Decomposed FC Layers in RNNs

Note that FC layers with the weight matrix $W \in \mathbb{R}^{M \times N}$ are ubiquitous in DNNs especially RNNs, and the parameters of FC layers account for a very high proportion of the total network parameters due to a large number of input and

output neurons. So the realization of compressing FC layers is of great significance for space complexity reduction. This section demonstrates the detailed process to compress FC layers up to reconstruct the whole LSTM into the HT format.

2.2.1. Tensorizing x and W

We tensorize the input vector x into a d -dimensional tensor \mathcal{X} to obtain high-dimensional representation of the input data, while W is transformed into a tensor with the same degree of dimensions for easier HT decomposition. These tensorization operations are essentially regrouping the data into $\mathcal{X} \in \mathbb{R}^{n_1 \times n_2 \times \dots \times n_d}$ and $\mathcal{W} \in \mathbb{R}^{m_1 \times m_2 \times \dots \times m_d \times n_d}$ with the constraints $M = \prod_{k=1}^d m_k$ and $N = \prod_{k=1}^d n_k$ (Novikov et al., 2015).

2.2.2. Compressing \mathcal{W}

Following Equation (2), (3) or (5), the d -dimensional tensor \mathcal{W} derived from the original matrix can be easily represented as the HT format. It should be emphasized that, although the normal form defined in Equation (3) is more used in the past, for the tensorizing weight \mathcal{W} , middle results produced by a serial of Kronecker products will cause heavy storage consumption, e.g., $U_1 \otimes U_2 \otimes \dots \otimes U_d$. This situation can even make the calculation process of compressed DNNs infeasible based on our practical experiences. Therefore, we prefer the basic form in Equation (2) and the contracted form in Equation (5) to compress weights in DNNs.

For the basic form, we reshape the transfer matrix $B_{12\dots d}$ and remove the Kronecker product of the first decomposition:

$$\begin{aligned} HT(\mathcal{W}) &= W_{1\dots d/2} B_{12\dots d} W_{(d/2+1)\dots d}^T \\ &= (W_{1\dots d/4} \otimes W_{(d/4+1)\dots d/2}) B_{12\dots d/2} B_{12\dots d} \\ &\quad B_{(d/2+1)\dots d}^T (W_{(d/2+1)\dots 3d/4} \otimes W_{(3d/4+1)\dots d})^T \quad (6) \\ &= \dots \end{aligned}$$

This process can significantly reduce the sizes of middle results, i.e., the result of Kronecker product of each two truncated matrices shall not be very large and it can be further reduced by contracting with the adjacent transfer matrix. For the contracted form, there is no need to preprocess some matrices, just to imitate Equation (5), we can have:

$$\begin{aligned} HT(\mathcal{W}) &= (\dots ((W_1 \times^1 B_{12} \times^1 W_2) \times^1 B_{1234} \times^1 \\ &\quad (W_3 \times^1 B_{34} \times^1 W_4)) \times^1 \dots \times^1 \quad (7) \\ &\quad (W_{(d-1)} \times^1 B_{(d-1)d} \times^1 W_d) \dots). \end{aligned}$$

According to Equation (6)-(7) and Figure 1, the relevant space complexity of weight can be heavily reduced from $\mathcal{O}((mn)^d)$ to $\mathcal{O}(dmnr + (d-1)r^3)$.

2.2.3. Computation between \mathcal{X} and HT Matrices

In the forward pass, the output of the HT-decomposed FC layer is obtained by the computation between the tensorized input \mathcal{X} and the stored decomposed matrices, i.e.,

W_i and B_i . In general there are two approaches to obtain the output, which are termed as *recovery computation* and *chain computation* respectively. The recovery computation is to recover the HT matrices to the corresponding original \mathcal{W} , and then multiply it by \mathcal{X} . The computation complexity of the recovery computation can be concluded as $\mathcal{O}((\log_2 d - 1)MN(r^3 + r^2))$ by using Equation (6).

Contrarily, the chain computation calculates the input with each truncated or transfer matrix in Equation (7) sequentially, because the operation between \mathcal{X} and \mathcal{W} is also contraction so that the appropriate order of contractions can be observed in the view of tensor network, e.g., Figure 2, where we perform the operations between the input and matrices in the so called *inorder traversal*, i.e., each time the input should be reshaped into a befitting matrix to satisfy its modes with the matrices to be contracted. The computation complexity of the chain computation is expressed as $\mathcal{O}((2d-1)n \max\{M, N\}r^{1+\log_2 d})$. In contrast, we find that the chain computation takes less time and is more suited for the forward pass, as the expensive MN is erased. Specifically, according to Equation (7), we can roughly rewrite the product Wx into the following form:

$$\phi(W, x) = \mathcal{X} \times^1 W_1 \times^1 B_{12} \times^1 W_2 \times^1 B_{1234} \times^1 \dots \times^1 W_d, \quad (8)$$

where $\phi(\cdot)$ means it is not a strict representation of Wx since the corresponding reshaping and transposing are omitted.

2.2.4. HT-Decomposed LSTM Model

Based on Equation (8), all kinds of FC layers in DNNs can be replaced with HT-decomposed ones for network compression. For example, long-short term memory (LSTM) (Hochreiter and Schmidhuber, 1997) is one of the advanced variants of RNNs, and its corresponding HT-decomposed version can be described as:

$$\begin{aligned} \Gamma_u &= \sigma(\phi(W_u, x_t) + \phi(R_u, a_{t-1}) + b_u), \\ \Gamma_f &= \sigma(\phi(W_f, x_t) + \phi(R_f, a_{t-1}) + b_f), \\ \Gamma_o &= \sigma(\phi(W_o, x_t) + \phi(R_o, a_{t-1}) + b_o), \\ \tilde{C}_t &= \tanh(\phi(W_c, x_t) + \phi(R_c, a_{t-1}) + b_c), \\ C_t &= \Gamma_u \odot \tilde{C}_t + \Gamma_f \odot C_{t-1}, \\ a_t &= \Gamma_o \odot \tanh(C_t), \end{aligned} \quad (9)$$

where σ and \tanh represent the sigmoid and hyperbolic function respectively, and W_θ ($\theta = u, f, o, c$) denotes the weight from the input to the hidden layer while R_θ presents the weight from the previous state to the next one.

2.3. HT-Decomposed Convolutional Kernels in CNNs

The convolutional kernel \mathcal{K} is the most crucial component of CNNs, and is harder to compress because of its inherent compactness. That is, parameters in \mathcal{K} are shared for different local fields of the input, and each parameter should be responsible for many different data resources. Even worse, this situation will be more severe if we compress the convolutional kernels to make their quantity of parameters lower.

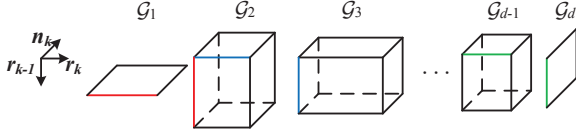


Figure 3: TT cores for a d -dimensional tensor. The special case is $r_0 = r_d = 1$. The same color represents the same dimensions which can be contracted.

Nonetheless, CNNs still need to be compressed for wider applications, since the modern CNNs appear to be very deep, e.g., ResNet-152 (He et al., 2016), so that the limited redundancy in convolutional kernels can be remitted to some extent in the view of the entire CNN (Denil et al., 2013).

In 2D-CNNs, the kernel $\mathcal{K} \in \mathbb{R}^{l \times l \times C \times S}$ might be decomposed in the HT format directly based on Figure 1. However, further tensorization should also be considered for better compression performance through theoretical analyses and experimental verification (Garipov et al., 2016), i.e., the convolutional kernel should be transformed into $\mathcal{K} \in \mathbb{R}^{l^2 \times c_1 s_1 \times c_2 s_2 \times \dots \times c_{d-1} s_{d-1}}$ with constraints $C = \prod_{k=1}^{d-1} c_k$ and

$S = \prod_{k=1}^{d-1} s_k$. Then the new tensor can be converted into the d truncated matrices and $d - 1$ transfer matrices according to Equation (6).

It should be emphasized that, although the chain computation in Equation (8) is faster than the recovery computation, the former can be hardly utilized in convolution since there is no associative law between convolution and contraction. Therefore, as the same as Garipov et al. (2016), we can just adopt the recovery computation for HT-decomposed convolutional kernels.

2.4. Relationship with TT

For a tensor $\mathcal{A} \in \mathbb{R}^{n_1 \times n_2 \times \dots \times n_d}$, Oseledets (2011) proposes TT decomposition which has a more regular format as (Lee and Cichocki, 2016):

$$\mathcal{A} = \mathcal{G}_1 \times^1 \mathcal{G}_2 \cdots \times^1 \mathcal{G}_d, \quad (10)$$

where $\mathcal{G}_k \in \mathbb{R}^{r_{k-1} \times n_k \times r_k}$ ($r_0 = r_d = 1$) shown in Figure 3 is termed as *core tensor*. In fact, TT decomposition is a specific variant of HT decomposition (Grasedyck and Lars, 2010; Grasedyck and Hackbusch, 2011; Lee and Cichocki, 2016). For example, in Equation (1), set t_l will have only one element if \mathcal{A} is in TT decomposition, and the following relationship should exist:

$$\mathcal{G}_k = \text{reshape}(U_{t_l} B_l), \quad (11)$$

where U_{t_l} will be kept on decomposing according to Equation (1). This process is shown in the right side of Figure 1 that presents as a degenerate tree, i.e., the TT format is the result of asymmetric HT decomposition and distinguishes from the HT format by the removal of Kronecker products and the formation of a uniform sequence of cores.

3. Hybrid Compression

In this section, we present and analyze the gradients of compressed DNNs in the HT and TT formats respectively. We conclude that the DNN in the HT format should achieve better performance than that in TT when the dimensions are balanced, and thus HT is more suited for compressing FC layers whose lengths of the dimensions could be balanced by more easy adjustment. However, we also discover that HT is more sensitive for unbalanced dimensions during training. Therefore, we propose a hybrid compression method that combines HT and TT together to separately compress FC layers and convolutional kernels of CNNs.

3.1. Gradient Analyses

3.1.1. Basic Definition

Error back propagation is usually applied in the training of DNNs. It is used to update the parameters by calculating the gradients which can be gained by the derivative of the error with respect to parameters. Thus, to discover the speciality of HT and TT in network compression, we focus on the gradients of compressed weights. For convenience, we uniformly use W_k to denote the truncated matrix U_k in HT or the matricized core tensor \mathcal{G}_k in TT.

In tensor-decomposed DNNs, the gradient of the terminal k th compressed weight W_k can be computed by the chain rule like:

$$\frac{\partial L}{\partial W_k} = \frac{\partial L}{\partial y} \frac{\partial y}{\partial W} \frac{\partial W}{\partial W_k}, \quad (12)$$

where L is the loss function, y is the output, and W denotes the uncompressed weight matrix. Apparently, different decomposition methods bring about the main differences on the third term in Equation (12), i.e., $\partial W / \partial W_k$. Besides, the descending distance of each updating depends on the product between gradient value and learning rate. For compressed matrices with the same initialization, in general the gradient with larger size can get more value which results in a longer descending distance of the matrix, so we also care about the size of the gradients.

3.1.2. Gradient of HT

It is known that in the HT dimension tree, any non-leaf node satisfies the relationship in Equation (4). For example, each corresponding minimum subtree at the last level in Figure 1 (left side) or Figure 2 can be represented as:

$$W_{(k-1)k} = W_{k-1} B_{(k-1)k} W_k, \quad (13)$$

where the neighbouring elements $k - 1$ and k ($k = 2, 4, 6, \dots, d$) belong to the dimensions of the minimum subtree. Accordingly, the gradient of each truncated matrix can be represented as:

$$\begin{cases} \frac{\partial W_{(k-1)k}}{\partial W_{k-1}} = [B_{(k-1)k} W_k] \otimes I_n, \\ \frac{\partial W_{(k-1)k}}{\partial W_k} = I_m \otimes [W_{k-1} B_{(k-1)k}]^T, \end{cases} \quad (14)$$

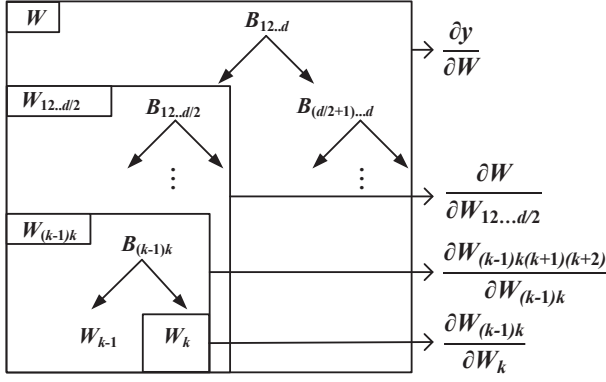


Figure 4: Partial derivatives in dimension tree. Each rectangle is regarded as a whole.

where n and m represent the row of W_{k-1} and W_k respectively. We adopt the chain rule shown in Figure 4 to compute the gradient of the uncompressed matrix W with respect to each HT truncated matrix W_k :

$$\frac{\partial W}{\partial W_k} = \frac{\partial W}{\partial W_{1\dots k\dots d/2}} \frac{\partial W_{1\dots k\dots d/2}}{\partial W_{1\dots k\dots d/4}} \dots \frac{\partial W_{(k-1)k}}{\partial W_k}, \quad (15)$$

where the number of partial derivatives is determined by the level of the dimension tree and reshaping is necessary for matrices due to the matricization of transfer tensors. For instance, for a three-level HT dimension tree, the gradient of W_1 should be:

$$\frac{\partial W}{\partial W_1} = \frac{\partial W}{\partial W_{12}} \frac{\partial W_{12}}{\partial W_1}, \quad (16)$$

where the dimension tree satisfies $W = W_{12}B_{1234}W_{34}$ and $W_{12} = W_1B_{12}W_2$. The gradient in Equation (16) can be derived from the rules in Equation (14), then the size of the gradient in Equation (15) is:

$$\text{size} \left(\frac{\partial W}{\partial W_k} \right) = r_k \times n_1 n_2 \dots n_{k-1} n_{k+1} \dots n_d. \quad (17)$$

3.1.3. Gradient of TT

For the network in the TT format, Novikov et al. (2015) derive the gradient of the output with respect to the core matrices (slices of the core tensors) of the TT-decomposed weights. To be more intuitive, we transfer the tensors to matrices and ignore the reshaping according to Equation (10), then the gradients of TT cores should be governed by:

$$\begin{cases} \frac{\partial W}{\partial W_1} = (W_2 W_3 \dots W_d) \otimes I_n, \\ \frac{\partial W}{\partial W_k} = (W_{k+1} W_{k+2} \dots W_d) \otimes (W_1 \dots W_{k-2} W_{k-1})^T, \\ \frac{\partial W}{\partial W_d} = I_m \otimes (W_1 W_2 \dots W_{d-1})^T, \end{cases} \quad (18)$$

where $k = 2, 3, \dots, d-1$, $n = n_1$, and $m = n_d$. The sizes of these gradients are:

$$\begin{cases} \text{size} \left(\frac{\partial W}{\partial W_1} \right) = n_1 r_1 \times n_1 n_2 \dots n_d, \\ \text{size} \left(\frac{\partial W}{\partial W_k} \right) = r_{k-1} r_k \times n_1 \dots n_{k-1} n_{k+1} \dots n_d, \\ \text{size} \left(\frac{\partial W}{\partial W_d} \right) = n_d r_{d-1} \times n_1 n_2 \dots n_d. \end{cases} \quad (19)$$

According to Equation (17) and (19), it is obvious that there is a certain difference between the gradients of HT and TT. The gradients of HT matrices have a unified form, while in TT the gradients are variable. The size of each gradient is largely related to dimensional lengths n that may have different effects on updating the matrix in HT and TT, which will be analyzed concretely in the following.

3.2. Gradient Transfer of Varying Dimensions

Previous experiments (Novikov et al., 2015) show that better compression performance can be achieved by tensorizing weight matrices into tensors with balanced length of dimensions. However, due to the fixed size of the filter, e.g., the most widely used 3×3 filter, the unbalanced dimensions will occur in the process of tensorization of convolutional kernels. Hence, in the following, we discuss two cases of HT and TT, i.e., equal and unequal length of dimensions, to analyze the effect on the performance of compressed DNNs based on gradient transfer.

3.2.1. Equal Length of Dimensions

We assume that there is a tensor $\mathcal{A} \in \mathbb{R}^{n_1 \times n_2 \times \dots \times n_{d-1} \times n_d}$ that satisfies $n_1 = n_2 = \dots = n_d = n$, and its every HT or TT rank equals n , which is also called mode-1 truncated rank produced by the matricization of $A^{(\{1\})}$ or $A^{(\{d\})}$ (Novikov et al., 2015; Wang et al., 2019). Therefore, for DNNs in the HT format, the size of each compressed truncated matrix shall be $n \times n$. However, matricized core tensors in the TT format are different because $r_0 = r_d = 1$, which means marginal core matrices W_1 and W_d have a different amount of information. This situation causes the gradients related to W_1 and W_d in TT-DNNs to be larger than those of other core matrices at the second dimension, i.e., $n^2 \times n^d$ in W_1 and W_d vs. $n^2 \times n^{d-1}$ in other matrices. To sum up, the unbalanced distribution of information and different updating rate of gradients might cause that the DNNs in the TT format have a lower precision than those in the HT format under the balanced dimension tree. In addition, this principle can also explain that TR, which is the same as TT except $r_0 = r_d \neq 1$, could achieve better compression performance than TT (Pan et al., 2018; Zhao et al., 2019).

3.2.2. Unequal Length of Dimensions

However, when the length of the p th dimension n_p of the tensor \mathcal{A} greatly decreases, gradients of compressed weights in HT and TT formats will have different changes. For HT, according to Equation (17), the size of $\partial W / \partial W_p$ is $r_p \times n_1 n_2 \dots n_{p-1} n_{p+1} \dots n_d$, which is larger than that of any

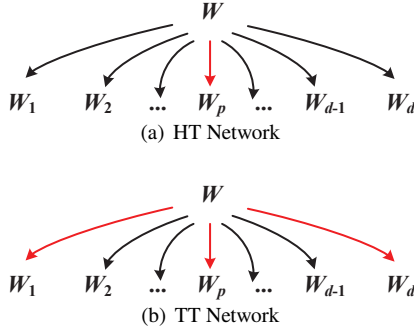


Figure 5: Gradient transfer in the compressed network when the unequal length occurs. n_p is smaller than others. The red arrow represents the larger value of the gradients in the gradient transfer.

other gradient due to the smaller term n_p . Then it brings a different updating rate of HT-truncated matrices with gradient transfer shown in Figure 5(a), where the value of gradient of the truncated matrix W_p is larger than others. As for TT, the sizes of the first and last gradients are also larger than others except the p th gradient $\partial W / \partial W_p$ according to Equation (19), and the gradient transfer in Figure 5(b) illustrates that more counts of larger gradients can be found compared with HT. Thus, it is apparent that the effects on the final performance of HT and TT should be different. For HT, unequal dimensions result in the consequence that the smaller matrix has a longer descending distance than others, while other matrices may update slower. The extremely unbalanced updating may make HT difficult to converge to the optimal solution and lead to poor performance. As for TT, different descending distances also exist, but there are more counts of matrices could update faster which makes TT more robust to unequal dimensions compared with HT, especially in the case of low degree of dimensions.

3.3. Hybrid Tensor Decomposition Strategy

The analyses above show that HT is more suited for compressing the tensor with balanced length of dimensions, while it is better for TT to compress the tensor with unbalanced dimensions. In practice, one can obtain the tensor with balanced dimensions more easily in FC layers (Novikov et al., 2015) rather than convolutional kernels since the latter generally have the fixed filter size (Garipov et al., 2016). For a network made up of different structures such as CNN, it is naturally not a good idea to compress the whole network with a single tensor decomposition method, either HT or TT. To this end, we propose a hybrid tensor decomposition strategy combining TT and HT together for CNNs consisting of convolutional kernels and FC layers. As depicted in Figure 6, HT and TT are respectively responsible for compressing their suitable structures, specifically convolutional kernels are decomposed in the TT format and weight matrices are stored in the HT format. We expect that the hybrid tensor decomposition may achieve better performance than only using the single method HT or TT.

4. Experiments

In this section, we will first aim at verifying the performance of HT-DNNs and comparing them with TT-DNNs to find whether HT is better for the weights with balanced dimensions. Then we emphasize the proposed hybrid tensor decomposition to compress 2D- and 3D-CNNs and check whether the hybrid strategy is better than either of HT or TT.

4.1. HT and TT Decomposition on RNNs and CNNs

In the following we will make a wide comparison between HT- and TT-DNNs, including RNNs and CNNs. Recently, some tensor decomposition practices have achieved outstanding performance on video classification such as TT-LSTM (Yang et al., 2017) and TR-LSTM (Pan et al., 2018). For this reason, we also choose LSTM as the reference network to classify UCF11 (Liu et al., 2009) and UCF50 (Reddy and Shah, 2012), which are two challenging video datasets. After that, we focus on the compression of convolutional kernels in CNNs based on the CIFAR-10 dataset (Krizhevsky, 2009) and adopt 3D-CNNs to recognize videos on UCF11 and CVRR-HANDS 3D datasets (Ohn-Bar and Trivedi, 2014). We use stochastic gradient descent (SGD) to train all of our networks from scratch with 0.9 momentum, and the learning rate is decayed 10 times per 30 epochs. This combination of hyper-parameters is a general selection in training process with SGD to some extent (Novikov et al., 2015; Brownlee, 2016; He et al., 2016).

4.1.1. Datasets and Training Details

UCF11 Dataset is also known as YouTube Action Data Set, which has 1600 video clips in total and includes 11 action categories. Each category is divided into 25 groups based on some common features, such as the same actor, similar background, similar viewpoint, and so on. Large variations of this dataset make it very challenging because of the different camera motion, object scale, viewpoint, etc. The dataset is processed differently for RNNs and CNNs in our experiments. In the experiments of compressing LSTM, we follow Yang et al. (2017) to randomly sample 6 RGB frames with size 160×120 from each clip and perform a 5-fold cross validation with mutual exclusive data splits. We use the LSTM which contains a hidden layer with 2304 neurons, and for tensorization, the input dimensions at each frame $160 \times 120 \times 3$ are reshaped to $15 \times 16 \times 16 \times 15$ and those of the hidden layer are $8 \times 6 \times 6 \times 8$. The initial learning rate is 0.001. For the experiments of compressing 3D-CNNs, we randomly extract 50 continuous RGB and optical flow frames with size 80×60 from each clip. Then the stacked RGB and optical flow frames are fed into the two stream CNNs and their tensorized forms (Wang et al., 2019), which is shown on the left side of Figure 7. The initial learning rate is still 0.001. However, we follow Wang et al. (2019) to select the leave one group to replace 5-fold cross validation since 3D-CNN might be more easily influenced by the similar background in the video clips of UCF11.

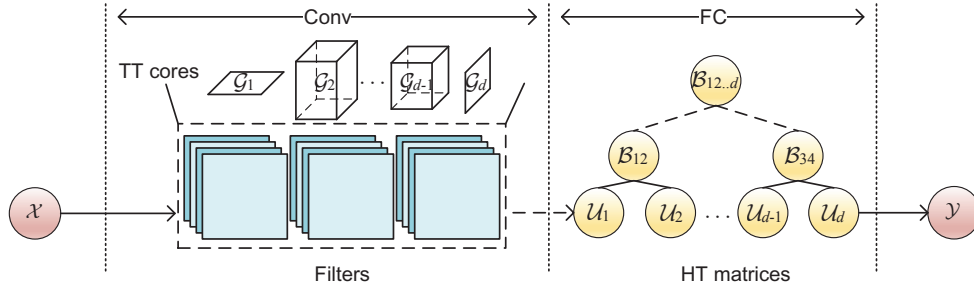


Figure 6: Illustration of the hybrid tensor decomposition of CNNs. The convolutional kernels are stored in the TT format and the dotted line surrounding the filters indicates the recovery computation of TT cores. The weight matrices of fully-connected layers are stored in the HT format.

UCF50 Dataset consists of 6681 video clips collected from YouTube. Here we just try the same LSTM that is also used on UCF11 dataset, and the training details are still the same without variation.

CIFAR-10 Dataset has a total number of 60000 32×32 colour images which can be split into 50000 training and 10000 validation samples, and is divided into 10 classes. We use VGG-19 (Simonyan and Zisserman, 2015), which is one of the best-performing CNNs on image recognition, as the reference model. We compress the convolutional kernels in the HT and TT formats respectively with the same ranks as 16, and the dimensions of tensorization depend on the channels, e.g., $64 = 4 \times 4 \times 4$, $128 = 4 \times 8 \times 4$, $256 = 4 \times 8 \times 8$, and $512 = 8 \times 8 \times 8$. The initial learning rate is 0.01.

CVRR-HANDS 3D (CVRR.) Dataset is also known as VIVA challenge’s hand gesture dataset which consists of 886 intensity and depth hand gesture videos. It is sampled by using a Kinect under real-world driving settings to study natural human activities, and 19 types of gestures performing 8 subjects inside a vehicle are collected. Following the existing practice (Molchanov et al., 2015), the dataset is expanded by mirroring and flipping in our experiment. For each video, we concatenate an intensity image, a depth image and a Sobel gradient image as a $28 \times 62 \times 3$ frame and make each video into uniform 32 frames as the final input. The referenced basic and compressed networks (Wang et al., 2019) we used consist of four 3-dimensional convolutional layers and two FC layers and the detailed architecture is shown on the right side of Figure 7. Comparing with the settings given by Wang et al. (2019), we add batch normalization after each FC layer. The initial learning rate is still 0.01.

4.1.2. Results of HT- and TT-decomposed Networks

To indicate the degree of compression, we term the ratio of uncompressed to compressed parameters of the same part as the compression factor (compr.). Specifically for CNNs, we follow Garipov et al. (2016) to indicate which part is compressed in TT or HT, e.g., ‘HT-Conv’ means the convolutional kernels are compressed in HT format. To ensure the reliability of the experimental results, we carried out 5 times for each training setting. The mean and standard devi-

Network for UCF11 Dataset	Network for CVRR-HANDS 3D Dataset
Input	
Conv3d-16 filter: 5×7×7	Conv3d-64 filter: 5×7×7
Maxpool3d: 4×4×4	Maxpool3d: 4×4×4
Conv3d-64 filter: 3×5×7	Conv3d-128 filter: 3×5×5
Maxpool3d: 4×4×4	Maxpool3d: 3×3×3
Conv3d-128 filter: 3×3×5	Conv3d-256 filter: 3×3×5
Maxpool3d: 2×2×3	Maxpool3d: 2×2×3
Conv3d-192 filter: 3×3×3	Conv3d-384 filter: 3×3×3
Maxpool3d: 4×4×4	Maxpool3d: 4×4×4
Conv3d-256 filter: 3×3×3	
Maxpool3d: 4×4×4	
FC-3125	
FC-1024	
Softmax	

Figure 7: Network configuration. Left: network for UCF11 dataset. Right: network for CVRR-HANDS 3D dataset.

ation of accuracy on these datasets are shown in Table 1.

The experiments indicate there are different advantages in HT and TT for compression, which also evidence our earlier theoretical analyses of gradients. The performances of UCF11 and UCF50 datasets show that RNNs in the HT format have better performance than those in the TT format when compressing weight matrices, though they are a bit worse than uncompressed RNNs. For the results in CNNs where only convolutional kernels are compressed, it is clear that the performances of TT-decomposed networks are closer to those of uncompressed networks, and HT-decomposed networks get the worst score with obvious accuracy loss. Overall, obviously the compressed CNNs present lower compression factor, which might be related to the compact structure of the convolution kernel.

4.2. Hybrid Tensor Decomposition on CNNs

The above experiments present the different performances in HT and TT compression of fully connected and

Table 1

Experimental results on several datasets to verify the performance of HT- and TT-decomposed networks.

Reference	Dataset	Baseline	Method	Compr.	Accuracy
LSTM	UCF11	79.81±2.78	HT-LSTM	58.41	79.69±2.13
			TT-LSTM	56.32	76.12±1.60
	UCF50	77.93±1.02	HT-LSTM	57.96	76.56±0.63
			TT-LSTM	55.91	75.13±0.47
CNN	UCF11	82.82±1.43	HT-Conv	8.49	81.50±2.01
			TT-Conv	8.49	82.43±2.24
	CIFAR-10	88.84±0.72	HT-Conv	4.29	83.66±0.58
			TT-Conv	4.29	87.27±0.29
	CVRR.	89.74±1.30	HT-Conv	7.37	86.90±2.51
			TT-Conv	7.37	88.16±1.78

Table 2

Verification of the networks in hybrid tensor decomposition strategy.

Dataset	Baseline	Method	Compr.	Accuracy
UCF11	82.82±1.43	HT-Conv-HT-FC	109.35	79.83±1.77
		TT-Conv-TT-FC	108.31	78.98±1.43
		Hybrid (ours)	106.26	80.60±1.90
CIFAR-10	88.84±0.72	HT-Conv-HT-FC	34.17	84.18±0.30
		TT-Conv-TT-FC	34.65	87.02±0.29
		Hybrid (ours)	36.18	87.75±0.37
CVRR.	89.74±1.30	HT-Conv-HT-FC	188.35	89.61±1.34
		TT-Conv-TT-FC	179.30	89.16±1.63
		Hybrid (ours)	171.38	90.00±1.70
ImageNet	58.56±0.62	HT-Conv-HT-FC	12.67	51.63±0.67
		TT-Conv-TT-FC	11.61	54.59±0.28
		Hybrid (ours)	11.61	55.01±0.13

convolutional layers. In the following, we severally adopt HT, TT and hybrid tensor decomposition for compressing the whole CNNs.

4.2.1. Datasets and Training Settings

Primary Verification. Our primary experimental verification is executed on the UCF11, CIFAR-10 and CVRR-HANDS 3D datasets following the previous training settings introduced in Section 4.1. The configuration of hyper-parameters of the fully connected layers and the convolutional layers of the hybrid decomposed networks are the same as the HT- and TT-decomposed networks, respectively.

Task on ImageNet. To the best of our knowledge, there are few works considering tensor-decomposed CNNs on large-scale datasets. In this experiment, we do further experiments on ImageNet 2012 dataset (Russakovsky et al., 2015), which roughly consists of 1.2 million training and 50,000 validation images with 1000 classes. The dataset was used in the competition called the ImageNet Large-Scale Visual Recognition Challenge (ILSVRC) and is still the focus of researchers nowadays. We choose the classical Alexnet (Krizhevsky et al., 2012) as the reference and compress the whole network in the HT, TT and hybrid formats,

respectively. The resized training images with the size of 256×256 are randomly cropped into 224×224 ones. We use the mini-batch of 128 and train the networks up to 100 epochs. The learning rate and the weight decay are selected to follow Krizhevsky et al. (2012). We exclude the dropout for the compressed networks to prevent under-fitting, and adopt the 224×224 center-crop in validation.

4.2.2. Results of Hybrid Tensor-decomposed CNNs

Like before, we use ‘HT-Conv-HT-FC’ to represent the CNN whose convolutional parts and fully connected parts are compressed in the HT format, and so does ‘TT-Conv-TT-FC’. We use ‘Hybrid’ to represent the network whose convolutional kernels are compressed in the TT format and fully connected weights are compressed in the HT format.

The results in Table 2 verify that the hybrid CNNs can achieve the best classification results among compressed ones. Particularly, the hybrid 3D-CNN on CVRR. even surpasses the uncompressed one. For the results on the large-scale dataset, the network in the simplex HT format is inferior due to the large proportion of convolutional layers. By contrast, the hybrid CNN still has the best performance among the compressed CNNs. For CIFAR-10 and ImageNet datasets, we also illustrate their corresponding

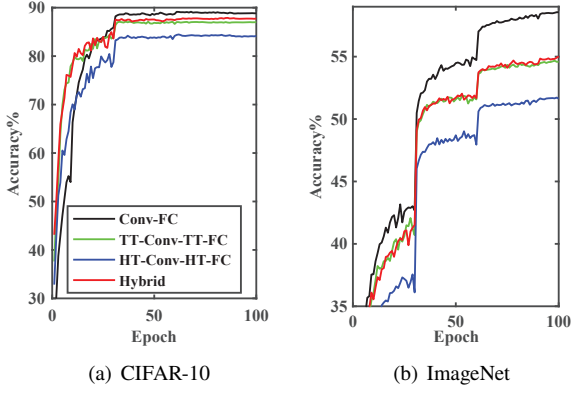


Figure 8: Training curves on CIFAR-10 and ImageNet datasets.

learning curves in Figure 8 as supplementary, which directly present the training processes of different networks and show the superior learning ability of hybrid CNNs. The learning ability of the HT-CNNs is obviously lagging behind other networks and the performance of hybrid CNNs improves on the basis of the TT-decomposed network.

5. Discussions

More and more compressed networks with low-rank factorization have been proposed, each of which has its own unique advantages but cannot suit any demands. Hence, a hybrid strategy is proposed in this paper. In this section we make some further analyses with the results of our experiments and extend to discussing some possible understanding of compressed networks.

5.1. Variable Length of Dimensions of HT

The experiments in section 4.1 present various performances of the HT-decomposed RNNs and CNNs, and imply that HT is more friendly to weight matrices because of the easier tensorization. In this subsection, we intuitively discuss the effect of variable length of dimensions in HT decomposition to verify and explain whether our gradient analyses in Section 3 are reasonable. We carefully design and train a network with two FC layers on MNIST dataset (LeCun et al., 1998) and resize the original images from 28×28 to 32×32 to facilitate the setting of experimental parameters. The network consists of two layers, in which the first weight matrix has the size of 1024×1024 and the second has the size 1024×10 . We only compress the first layer as a 4-dimensional tensor and train several times with different settings of dimensions and ranks.

The curves in Figure 9 present the comparison between balanced dimensions and unbalanced dimensions of the HT-decomposed network and indicate that the former style can get the best accuracy, thus our gradient analyses of HT is supported. Additionally, the compression factor of the balanced dimensions is higher than any other unbalanced dimensions. That is, when the same rank is taken, the parameters of the balanced dimensions will be fewer. Besides,

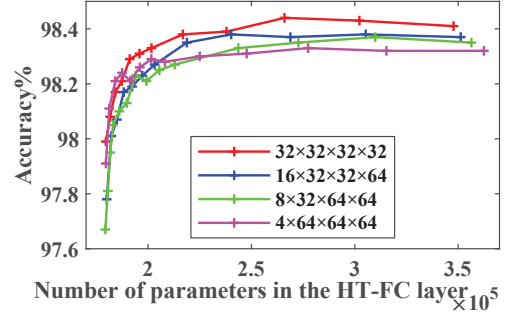


Figure 9: Experiment of examining the relationship between performance and shapes on the MNIST dataset. The legends represent different weight sizes of the HT-FC layer after tensorization.

the curves reflect that the performance of a compressed network will no longer improve when the number of parameters reaches a certain degree. Another point should be emphasized is that, in conditions of fewer parameters, there is only a slight difference of performances between the network with balanced dimensions and other designs. Therefore, choosing appropriate ranks is important to fully express the ability of network compression. Based on these experiences, we suggest to select the largest dimension length as the HT ranks, i.e., the largest mode-1 truncated rank.

5.2. Superiority of Hybrid Strategy

We have briefly introduced the superiority of hybrid strategy in the last section based on our experimental results. Here we would like to further explain some comprehensive phenomena to afford a more completed representation.

5.2.1. Variant Compr. under the Same Ranks

According to the experiments of LSTMs recorded in Table 1, we discover that different networks have various compression factors under the same ranking rule. HT-LSTM saves more memory under the same experimental settings compared with TT-LSTM, and the former even gets higher accuracy. This is completely accorded with the gradients analysis and corresponding experimental verification in Figure 9. Therefore, replacing the TT-FC layer with HT-FC layer in CNNs becomes a natural selection, and the experimental results in Table 2 confirms this. On the other hand, since the HT is sensitive to unbalanced dimensions, HT-Conv appears to be an unadvisable choice.

5.2.2. Adaptability on Convolutional Kernels

According to Table 1, it is undoubted that HT is sensitive to unbalanced dimensions so that HT-Conv is not a sensible choice, which is also consistent with our gradient analysis in Section 3. However, for 3D-CNNs, the results of HT-Conv-HT-FC even exceed those of TT-Conv-TT-FC on UCF11 and CVRR. datasets. The probable reason might be that the tensorizing shapes of 2D- and 3D-convolutional kernels are different, and more importantly, this difference has potential influence on gradient transfer.

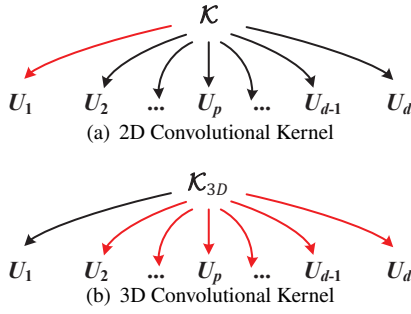


Figure 10: Gradient transfer of 2D- and 3D-convolutional kernels in HT format. The red arrow represents the larger value of the gradients in the gradient transfer.

In detail, the 3D-convolutional kernel has a cubic filter, thus the corresponding tensorization should be $\mathcal{K}_{3D} \in \mathbb{R}^{wht \times c_1 s_1 \times c_2 s_2 \times \dots \times c_d s_d}$, where w , h and t are filter sizes. Combining with the design of 3D-CNNs in Figure 7, it can be noticed that usually there is $wht > c_i s_i$ ($i = 1, 2, \dots, d$). Contrarily, most 2D-convolutional kernels have the filter size of 3×3 , which often results in $l^2 < c_i s_i$, since c_i or s_i is larger than 4 under most circumstances. According to the gradient transfer of HT illustrated in Figure 5(a), the larger portion of gradient from W will be attracted by the smaller mode l^2 , so many parameters in the compressed 2D-convolutional kernels could just be updated finitely. However, for 3D-convolutional kernels, smaller modes are all the $c_i s_i$ so that the situation is opposite to 2D-convolutional kernels, then the gap between TT- and HT-decomposed 3D-CNNs is shrunk. Figure 10 illustrates this difference vividly.

Even so, HT still can not surpass TT in performance if we only compress convolutional kernels in 3D-CNNs. Nevertheless, combining with the advantages of HT-FC part, 3D-CNNs in pure HT format runs better than TT, let alone the hybrid CNNs.

5.2.3. Layer Coupling

Our results also indicate that compressing the whole CNN in hybrid tensor-decomposed format is better than only compressing convolutional kernels according to Table 1 and 2. For example, when compressing two parts of CNN on the CIFAR-10 dataset, the accuracy can be improved from only compressing convolutional kernels even the former has fewer parameters. The reason is that there exists coupling between different parts of CNNs, i.e., compressing the entire CNN will not be much worse than only compressing convolutional or FC part (Wang et al., 2019). Another interesting phenomenon is that the CNN in HT format could surpass the one in TT format sometimes when the entire CNN is compressed, e.g., our results on UCF11 and CVRR. datasets, which is explained in the last subsection above.

5.3. Influence of Tensor Structure on Complexity

In this paper we mainly present the compressed networks with two treelike decomposition structures, i.e., HT and TT. Here we concretely discuss some differences of space

and computation complexity among multiple decomposition methods but not limited to HT and TT.

The stored format of parameters in compressed networks determines the space and computation complexity. We summarize the computation and space complexity of HT and TT in Table 3, and in addition, those of TR and BTM are also given for a comprehensive comparison. For the space complexity, all of these compression methods can greatly reduce the number of parameters in comparison with uncompressed networks. Due to r^3 , the complexity of HT seems to be higher under the same and larger rank, but more information might be retained under the same amount of parameters because the rank required by HT could be smaller in this situation according to Grasedyck and Hackbusch (2011). The large memory also occurs in BTM. However, TR has the most special space complexity since its tensorization is usually treated as a $2d$ - rather than d -dimensional tensor (Zhao et al., 2019; Pan et al., 2018), i.e., $\mathcal{W} \in \mathbb{R}^{m_1 \times m_2 \times \dots \times m_d \times n_1 \times n_2 \times \dots \times n_d}$, which is very effective to cut down the dimensional length. Generally speaking, for a fixed matrix $W \in \mathbb{R}^{M \times N}$, higher d results in lighter space complexity. When dimensional lengths are reduced to mn/p , the new dimension shall rise to $d \log_{mn/p} mn$. It is obvious that the product of dimensions $d \log_{mn/p} mn$ and dimensional lengths mn/p has dropped, which leads to the lower space complexity.

In the aspect of running time, the simple and unified format like the TT can greatly reduce the computation complexity due to the advantages of sequenced contractions through each core tensor in the forward pass (Novikov et al., 2015). While the low correlation between the truncated matrices in HT (truncated matrices should be connected by transfer matrices) results in higher computation complexity, which is also more sensitive to rank. For TR whose computation complexity is close to HT, since its specific tensorizing strategy as we mentioned, the computation complexity is still higher than that of TT even the product MN is avoided. With respect to BTM, the computation complexity should be the highest because of its exponential sensitive to ranks.

All in all, TT is derived from the HT degenerate tree, and has lower flexibility than HT but is simple to calculate in DNNs. Meanwhile, the advantage of HT is its potential of maintaining information under the same level of space complexity (ranks may be different). Besides, TR is a relatively particular case whose space complexity might be smaller but computation complexity is higher, and BTM has no advantage in terms of complexity.

5.4. Deeper Understanding of Tensor-decomposed DNNs

In general, compressed networks are considered to be derived from uncompressed networks, and the generated accuracy loss usually exists. In our experiments, most of results show that the classification ability of the compressed network declines as well. However, the performance of the compressed network may far exceed that of uncompressed networks in some specific cases (Pan et al., 2018; Yang et al.,

Table 3

Comparison among uncompressed FC layer, HT-FC layer, TT-FC layer, TR-FC layer and BT-D-FC layer on forward computation and space complexity. The baseline is derived from the weight matrix $W \in \mathbb{R}^{M \times N}$, $N = n_1 \times n_2 \times \dots \times n_d$, n is the maximal $n_k (k = 1, 2, \dots, d)$, $M = m_1 \times m_2 \times \dots \times m_d$, m is the maximal $m_k (k = 1, 2, \dots, d)$, r is the maximal rank and C is the CP-rank.

Method	Computation	Space
FC	$\mathcal{O}(MN)$	$\mathcal{O}(MN)$
HT format	$\mathcal{O}((2d-1)n \max\{M, N\}r^{1+\log_2 d})$	$\mathcal{O}(dmnr + (d-1)r^3)$
TT format	$\mathcal{O}(dn \max\{M, N\}r^2)$	$\mathcal{O}((d-2)mnr^2 + 2mnr)$
TR format	$\mathcal{O}(d(M+N)r^3)$	$\mathcal{O}(d(m+n)r^2)$
BTD format	$\mathcal{O}(dn \max\{M, N\}r^d C)$	$\mathcal{O}((dmnr + r^d)C)$

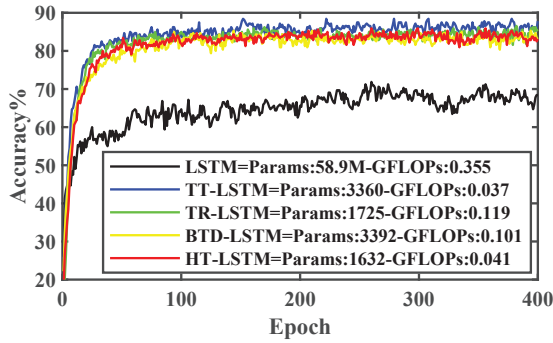


Figure 11: Performance of different LSTMs with 256 hidden neurons on the UCF11 dataset.

2017; Ye et al., 2017), which appears to be very counter-intuitive. We change the number of neurons of the hidden layer of LSTM in section 4.1 from 2304 to 256 in the light of previous network configurations (Pan et al., 2018; Yang et al., 2017; Ye et al., 2017) and train the uncompressed, TT-, HT-, TR- and BTD-LSTMs on UCF11 dataset successively. For the compressed networks except TR, the input dimensions are reshaped to $8 \times 20 \times 20 \times 18$ and the output dimensions are $4 \times 4 \times 4 \times 4$. The hyper-parameters of TR-LSTM follows (Pan et al., 2018) and other experimental settings are the same as (Yang et al., 2017).

The corresponding best learning curves in Figure 11 present the outstanding ability of compressed LSTMs obviously, i.e., the accuracy of any kind of compressed LSTM is greatly improved from the uncompressed one. Moreover, as we use the Adam optimizer here by following Pan et al. (2018); Yang et al. (2017); Ye et al. (2017), the long-term performances fluctuate slightly, where each compressed LSTM is more stable than that of uncompressed one, although there are a little differences in these compressed LSTMs. Comparing the results in Table 1, the uncompressed LSTM here has poor fitting ability due to its less hidden neurons, however, all the compressed LSTMs achieve much better performance with fewer parameters and faster operations.

We deem that all these results indicate that the tensor-decomposed network can be regarded as a new network that is independent of the original uncompressed network

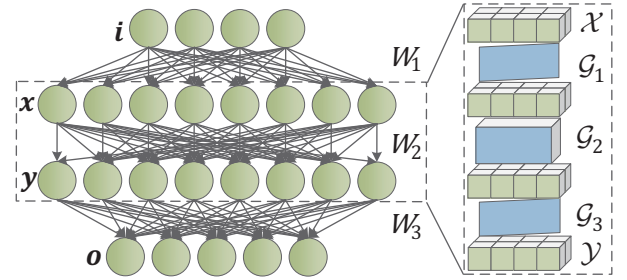


Figure 12: An example demonstrating that the tensor-decomposed network can be regarded as a new network that is independent of the uncompressed network to some extent. Here a network with three layers of weights could be restructured as a new one with five layers of weights by TT. Two layers of hidden neurons turn into four layers.

to some extent. In general the compressed DNN is hardly to surpass the relevant original one, unless redesign a new compact neural architecture, e.g., neural architecture search (NAS) (Deng et al., 2020). That is to say, the tensor architecture has ability to reconstruct the topology of neurons, or even describe and explain the potential mechanism of DNNs (Cichocki, 2018). Taking TT as an example because of its simplicity, a new and compact network could be constructed based on the original one as shown in Figure 12, if we ignore that there is no nonlinear activation functions among the dotted box. In a sense, the tensor-decomposed DNN changes the original architecture of uncompressed network, since the new data flow is produced, particularly the chain computation of HT or the sequenced contractions of TT (Novikov et al., 2015) is utilized. By contrast, quantization and pruning do not have the similar characteristic, i.e., it is difficult for them to abandon their correlated uncompressed DNNs. Consequently, this situation implies that the tensor decomposition method might be perpendicular to quantization and pruning, and forebodes the promising joint-way compression based on these different methods in future.

6. Conclusion

In this paper, we apply HT decomposition with the balanced pattern to compress RNNs and CNNs for the first time, and propose a new hybrid compression strategy to improve

the performance of tensor-decomposed CNNs. With tens of times the compression factor, the accuracy is approximately maintained, which indicates that high redundancy in the original network can be weakened through the proposed method.

We also compare the HT format with the TT format that originates from the unbalanced pattern of HT decomposition. One important finding is that the HT format is more suited for compressing weight matrices and the TT format has advantages on compressing convolutional kernels. The proposed hybrid compression based on different advantages of HT and TT formats shows advanced overall performance. These results contribute to choosing the best strategy for neural network compression and make a step forward in deploying neural networks on embedded devices.

Last but not least, we would like to note that there are various other techniques having been proposed to compress DNNs in recent years, such as data quantization (Vanhoucke and Mao, 2011; Wu et al., 2018), network sparsification (Sutskever et al., 2014; Zhu and Gupta, 2018) and neural architecture search (Zoph et al., 2018; Zoph and Le, 2017). In this work, we only focus on the hybrid tensor decomposition method by decomposing large-scale parameter representation into a series of smaller tensors to shrink the memory volume and operation number. For the future work, we believe that the joint-way compression across multiple techniques to pursue an extreme compression factor is of great potential.

Acknowledgement

This work is partially supported by National Key R&D Program of China (No.2018YFE0200200), Beijing Academy of Artificial Intelligence (BAAI), and a grant from the Institute for Guo Qiang, Tsinghua university, and key scientific technological innovation research project by Ministry of Education, and the open project of Zhejiang laboratory.

References

- Brownlee, J., 2016. Using learning rate schedules for deep learning models in python with keras. <https://machinelearningmastery.com/using-learning-rate-schedules-deep-learning-models-python-keras/>.
- Carroll, J.D., Chang, J.J., 1970. Analysis of individual differences in multidimensional scaling via an n-way generalization of the Tucker decomposition. *Psychometrika* 35, 283–319.
- Chen, Q., Zhu, X., Ling, Z.H., Wei, S., Jiang, H., Inkpen, D., 2017. Enhanced lstm for natural language inference, in: Proceedings of the 55th Annual Meeting of the Association for Computational Linguistics, pp. 1657–1668.
- Cichocki, A., 2018. Tensor networks for dimensionality reduction, big data and deep learning, in: Advances in Data Analysis with Computational Intelligence Methods. Springer International Publishing AG. volume 738 of *Studies in Computational Intelligence*, pp. 3–49.
- Cohen, N., Sharir, O., Shashua, A., 2016. On the expressive power of deep learning: A tensor analysis. *Journal of Machine Learning Research: Workshop and Conference Proceedings* 49, 1–31.
- Cohen, N., Shashua, A., 2016. Convolutional rectifier networks as generalized tensor decompositions, in: Proceedings of the 33rd International Conference on Machine Learning, pp. 955–963.
- De Lathauwer, L., 2008. Decompositions of a higher-order tensor in block terms — Part II: Definitions and uniqueness. *SIAM Journal on Matrix Analysis and Applications* 30, 1033–1066.
- Deng, C., Sun, F., Qian, X., Lin, J., Wang, Z., Yuan, B., 2019. Tie: Energy-efficient tensor train-based inference engine for deep neural network, in: 2019 Conference on International Symposium on Computer Architecture, pp. 264–278.
- Deng, L., Li, G., Han, S., Shi, L., Xie, Y., 2020. Model compression and hardware acceleration for neural networks: A comprehensive survey. *Proceedings of the IEEE* 108, 485–532.
- Denil, M., Shakibi, B., Dinh, L., Ranzato, M., Freitas, N.d., 2013. Predicting parameters in deep learning, in: Proceedings of the 26th International Conference on Neural Information Processing Systems (NIPS), pp. 2148–2156.
- Espig, M., Hackbusch, W., Handschuh, S., Schneider, R., 2011. Optimization problems in contracted tensor networks. *Computing and Visualization in Science* 14, 271–285.
- Garipov, T., Podoprikin, D., Novikov, A., Vetrov, D., 2016. Ultimate tensorization: compressing convolutional and fc layers alike. *arXiv:1611.03214*.
- Grasedyck, Lars, 2010. Hierarchical singular value decomposition of tensors. *Siam Journal on Matrix Analysis and Applications* 31, 2029–2054.
- Grasedyck, L., Hackbusch, W., 2011. An introduction to hierarchical (h-) rank and tt-rank of tensors with examples. *Computational Methods in Applied Mathematics* 11, 291–304.
- Hackbusch, W., Kijhn, S., 2009. A new scheme for the tensor representation. *Journal of Fourier Analysis and Applications* 15, 706–722.
- He, K., Zhang, X., Ren, S., Sun, J., 2016. Deep residual learning for image recognition, in: 2016 IEEE Conference on Computer Vision and Pattern Recognition.
- Heess, N., Hunt, J.J., Lillicrap, T.P., Silver, D., 2015. Memory-based control with recurrent neural networks, in: NIPS Deep Reinforcement Learning Workshop 2015.
- Hinton, G., Vinyals, O., Dean, J., 2014. Distilling the knowledge in a neural network, in: NIPS Deep Learning Workshop.
- Hitchcock, F.L., 1927. The expression of a tensor or a polyadic as a sum of products. *Studies in Applied Mathematics* 6, 164–189.
- Hochreiter, S., Schmidhuber, J., 1997. Long short-term memory. *Neural Computation* 9, 1735–1780.
- Hou, M., Chaib-draa, B., 2015. Hierarchical tucker tensor regression: Application to brain imaging data analysis, in: IEEE International Conference on Image Processing, pp. 1344–1348.
- Huang, H., Yu, H., 2018. Lttn: A layerwise tensorized compression of multilayer neural network. *IEEE Transactions on Neural Networks and Learning Systems*, 1–15.
- Kim, Y.D., Park, E., Yoo, S., Choi, T., Yang, L., Shin, D., 2016. Compression of deep convolutional neural networks for fast and low power mobile applications, in: Proceedings of the International Conference on Learning Representation.
- Kressner, D., Tobler, C., 2011. Preconditioned low-rank methods for high-dimensional elliptic PDE eigenvalue problems. *Computational Methods in Applied Mathematics* 11, 363–381.
- Kressner, D., Tobler, C., 2014. Algorithm 941: Htucker—a matlab toolbox for tensors in hierarchical tucker format. *ACM Transactions on Mathematical Software* 40, 22.1–22.22.
- Krizhevsky, A., 2009. Learning multiple layers of features from tiny images. Master's thesis, Computer Science Department, University of Toronto.
- Krizhevsky, A., Sutskever, I., Hinton, G., 2012. Imagenet classification with deep convolutional neural networks. *Proceedings of the Neural Information Processing Systems* 1, 1097–1105.
- Lebedev, V., Ganin, Y., Rakhuba, M., Oseledets, I., Lempitsky, V., 2015. Speeding-up convolutional neural networks using fine-tuned cp-decomposition, in: Proceedings of the International Conference on Learning Representation.
- LeCun, Y., Cortes, C., Burges, C.J., 1998. The mnist database of handwritten digits. URL: <http://yann.lecun.com/exdb/mnist/>.
- Lee, N., Cichocki, A., 2016. Regularized computation of approximate pseu-

- doinverse of large matrices using low-rank tensor train decompositions. *SIAM Journal on Matrix Analysis and Applications* 37, 598–623.
- Liu, J., Luo, J., Shah, M., 2009. Recognizing realistic actions from videos, in: *IEEE Conference on Computer Vision and Pattern Recognition*.
- Mnih, V., Kavukcuoglu, K., Silver, D., et al., 2015. Human-level control through deep reinforcement learning. *Nature* 518, 529–533.
- Molchanov, P., Gupta, S., Kim, K., Kautz, J., 2015. Hand gesture recognition with 3D convolutional neural networks, in: *IEEE Conference on Computer Vision and Pattern Recognition Workshops*, pp. 1–7.
- Novikov, A., Podoprikin, D., Osokin, A., Vetrov, D., 2015. Tensorizing neural networks, in: *Proceedings of the Neural Information Processing Systems*.
- Ohn-Bar, E., Trivedi, M.M., 2014. Hand gesture recognition in real time for automotive interfaces: A multimodal vision-based approach and evaluations. *IEEE Transactions on Intelligent Transportation Systems* 15, 2368–2377.
- Oseledets, I., 2011. Tensor-train decomposition. *SIAM J. Scientific Computing* 33, 2295–2317.
- Pan, Y., Xu, J., Wang, M., Ye, J., Wang, F., Bai, K., Xu, Z., 2018. Compressing recurrent neural networks with tensor ring for action recognition, in: *Proceedings of the Neural Information Processing Systems*.
- Reddy, K.K., Shah, M., 2012. Recognizing 50 human action categories of web videos. *Machine Vision and Applications* 24, 971–981.
- Russakovsky, O., Deng, J., Su, H., Krause, J., Satheesh, S., Ma, S., Huang, Z., Karpathy, A., Khosla, A., Bernstein, M., Berg, A.C., Fei-Fei, L., 2015. Imagenet large scale visual recognition challenge. *International Journal of Computer Vision* 115, 211–252.
- Simonyan, K., Zisserman, A., 2015. Very deep convolutional networks for large-scale image recognition, in: *Proceedings of the International Conference on Learning Representation*.
- Srinivas, S., Babu, R.V., 2015. Data-free parameter pruning for deep neural networks, in: *IEEE Conference on Computer Vision and Pattern Recognition*, pp. 2830–2838.
- Sutskever, I., Vinyals, O., Le, Q.V., 2014. Sequence to sequence learning with neural networks, in: *Proceedings of the Neural Information Processing Systems*.
- Tucker, L., 1966. Some mathematical notes on three-mode factor analysis. *Psychometrika* 31, 279–311.
- Vanhoeck, V., Mao, M., 2011. Improving the speed of neural networks on cpus, in: *NIPS Deep Learning and Unsupervised Feature Learning Workshop*.
- Wang, D., Zhao, G., Li, G., Deng, L., Wu, Y., 2019. Lossless compression for 3dcnns based on tensor train decomposition. *arXiv:1912.03647*.
- Wu, B., Iandola, F., Jin, P.H., Keutzer, K., 2017. Squeezednet: Unified, small, low power fully convolutional neural networks for real-time object detection for autonomous driving, in: *IEEE Conference on Computer Vision and Pattern Recognition*.
- Wu, S., Li, G., Chen, F., Shi, L., 2018. Training and inference with integers in deep neural networks, in: *Proceedings of the International Conference on Learning Representation*.
- Yang, Y., Krompass, D., Tresp, V., 2017. Tensor-train recurrent neural networks for video classification, in: *Proceedings of the International Conference on Machine Learning*.
- Ye, J., Wang, L., Li, G., Chen, D., Zhe, S., Chu, X., Xu, Z., 2017. Learning compact recurrent neural networks with block-term tensor decomposition. *arXiv:1712.05134*.
- Zhao, Q., Sugiyama, M., Cichocki, A., 2019. Learning efficient tensor representations with ring-structured networks, in: *IEEE International Conference on Acoustics, Speech and Signal Processing*, pp. 8608–8612.
- Zhu, M.H., Gupta, S., 2018. To prune, or not to prune: Exploring the efficacy of pruning for model compression, in: *Proceedings of the International Conference on Learning Representation*.
- Zoph, B., Le, Q.V., 2017. Neural architecture search with reinforcement learning, in: *Proceedings of the International Conference on Learning Representation*.
- Zoph, B., Vasudevan, V., Shlens, J., Le, Q.V., 2018. Learning transferable architectures for scalable image recognition, in: *2018 IEEE/CVF Conference on Computer Vision and Pattern Recognition (CVPR)*.